ANNALS of Clinical and Translational Neurology
Open Access
AMERICAN NEUROLOGICAL ASSOCIATION

RESEARCH ARTICLE

Recurrent seizure-related *GRIN1* variant: Molecular mechanism and targeted therapy

Yuchen Xu[1,2], Rui Song[1,2], Wenjuan Chen[1,†], Katie Strong[1], Daniel Shrey[3,4], Satyanarayana Gedela[5], Stephen F. Traynelis[1,6], Guojun Zhang[5,*] & Hongjie Yuan[1,6,*]

[1]Department of Pharmacology and Chemical Biology, Emory University School of Medicine, Atlanta, Georgia
[2]Department of Neurology, Xiangya Hospital, Central South University, Changsha, Hunan, China
[3]Division of Neurology, Children's Hospital of Orange County, Orange, California
[4]Department of Pediatrics, University of California Irvine, Irvine, California
[5]Division of Neurology, Department of Pediatrics, Emory University School of Medicine, Atlanta, Georgia
[6]Center for Functional Evaluation of Rare Variants (CFERV), Emory University School of Medicine, Atlanta, Georgia

Correspondence
Guojun Zhang and Hongjie Yuan, Department of Pharmacology and Chemical Biology, Emory Univ. School of Medicine, Rollins Research Center, 1510 Clifton Road, Atlanta GA 30322-3090. Tel: 404-727-1375; Fax: 404-727-0365; E-mail: guojun.zhang@emory.edu; hyuan@emory.edu

Present address
[†]Department of Psychiatry, Sir Run Run Shaw Hospital, Zhejiang University School of Medicine, Hangzhou, China

Funding Information
This work was supported by the NIH (R35 NS111619 to SFT, R01 HD082373 to H.Y.) and Austin's Purpose.

Received: 5 April 2021; Revised: 20 May 2021; Accepted: 24 May 2021

***Annals of Clinical and Translational Neurology* 2021; 8(7): 1480–1494**

doi: 10.1002/acn3.51406

*These authors contributed equally to this work.

Abstract

Objective: Genetic variants in the *GRIN* genes that encode N-methyl-D-aspartate receptor (NMDAR) subunits have been identified in various neurodevelopmental disorders, including epilepsy. We identified a *GRIN1* variant from an individual with early-onset epileptic encephalopathy, evaluated functional changes to NMDAR properties caused by the variant, and screened FDA-approved therapeutic compounds as potential treatments for the patient. **Methods**: Whole exome sequencing identified a missense variant in *GRIN1*. Electrophysiological recordings were made from *Xenopus* oocytes and transfected HEK cells to determine the NMDAR biophysical properties as well as the sensitivity to agonists and FDA-approved drugs that inhibit NMDARs. A beta-lactamase reporter assay in transfected HEK cells evaluated the effects of the variant on the NMDAR surface expression. **Results**: A recurrent de novo missense variant in *GRIN1* (c.1923G>A, p.Met641Ile), which encodes the GluN1 subunit, was identified in a pediatric patient with drug-resistant seizures and early-onset epileptic encephalopathy. In vitro analysis indicates that GluN1-M641I containing NMDARs showed enhanced agonist potency and reduced Mg^{2+} block, which may be associated with the patient's phenotype. Results from screening FDA-approved drugs suggested that GluN1-M641I containing NMDARs are more sensitive to the NMDAR channel blockers memantine, ketamine, and dextromethorphan compared to the wild-type receptors. The addition of memantine to the seizure treatment regimen significantly reduced the patient's seizure burden. **Interpretation**: Our finding contributes to the understanding of the phenotype–genotype correlations of patients with *GRIN1* gene variants, provides a molecular mechanism underlying the actions of this variant, and explores therapeutic strategies for treating *GRIN1*-related neurological conditions.

INTRODUCTION

N-methyl-D-aspartate receptors (NMDARs) are ligand-gated ion channels that mediate a slow component of excitatory synaptic transmission in the brain. Functional NMDARs are hetero-tetrameric assemblies of two GluN1 subunits (encoded by *GRIN1*) and two GluN2 subunits, of which there are four types (A-D, encoded by *GRIN2A-D*).[1,2] Different GluN subunits show differential spatial and developmental expression profiles, as well as various biological properties. For example, GluN1 is expressed ubiquitously, whereas GluN2B and GluN2D subunits are predominantly expressed prenatally and GluN2A and GluN2C subunit expression increases postnatally.[3,4] All NMDAR subunits share a similar architecture. The extracellular portion consists of an amino-

© 2021 The Authors. *Annals of Clinical and Translational Neurology* published by Wiley Periodicals LLC on behalf of American Neurological Association
This is an open access article under the terms of the Creative Commons Attribution-NonCommercial-NoDerivs License, which permits use and distribution in any medium, provided the original work is properly cited, the use is non-commercial and no modifications or adaptations are made.

terminal domain (NTD, also known as ATD), which contains binding sites for modulators, and an agonist-binding domain harboring binding sites for glutamate or glycine. Three transmembrane domains M1, M3, M4, and a re-entrant pore-forming loop M2 associate together to form the channel pore. The C-terminal domain is involved in intracellular signaling.[1,2] The activation of NMDARs requires the occupation of two glycine-binding sites on GluN1 and two glutamate-binding sites on GluN2, which trigger the opening of a cation-selective pore. This action mediates an inward current flux with neuronal depolarization and a subsequent increase in intracellular Ca^{2+} concentration.[5] In addition, extracellular modulators, such as Mg^{2+} and protons, regulate NMDARs negatively.[1,2,6]

NMDARs play an essential role in normal brain function such as learning, memory, and synaptic plasticity. The malfunction of NMDARs has been proposed to associate with a wide range of pathological conditions.[1,2,4,7,8] De novo *GRIN1* variants have been identified in a set of neurological diseases, including developmental delay, intellectual disability, epilepsy, autism-spectrum disorders, hypotonia, and movement disorders.[2,9-16] The rapid technical advances in next-generation whole-exome sequencing have increased the number of diseased-related *GRIN* variants identified.[2] Loss-of-function and gain-of-function missense variants have been identified[2,16]; the functional consequences are not necessarily clear a priori without functional testing. However, there is a lag in the functional evaluation of how these variants influence NMDAR function, which limits both our understanding of the mechanisms underlying the patients' phenotypes as well as the potential therapeutic options.

In this study, we report a de novo *GRIN1* missense variant that results in an amino acid substitution in the GluN1 subunit (c.1923G>A, p.Met641Ile). The variant was identified in a male pediatric patient with early-onset epileptic encephalopathy and severe developmental delay. Comprehensive functional investigation revealed that the variant altered the NMDAR agonist potency, sensitivity to Mg^{2+} inhibition, channel open probability, and surface trafficking. Since the patient's seizures were resistant to anti-seizure medicines, we evaluated the potency of FDA-approved NMDAR blockers, and found the variant increased channel blocker potency compared to wild-type (WT) receptors. Following a discussion of the risks and benefits, the family of the individual was offered off-label treatment with memantine, which significantly reduced the seizure burden. Our results reveal the complex effects that a *GRIN1* variant can exert on NMDAR function, which ultimately contributed to our patient's phenotype. Moreover, the success of this single-subject trial highlights the potential of precision medicine.

SUBJECTS/MATERIALS AND METHODS

Consent, study approvals, and diagnostic workup

All studies in this paper were conducted according to the guidelines of Emory University and approved by the Emory University IRB. The written informed consent from the patient's parents was obtained before the study. Whole-exome sequencing of the patient and his biological parents was performed using clinical next-generation sequencing (Invitae Genetic Testing, San Francisco, CA). The pathogenicity prediction was performed according to the ACMG guidelines 2015.[17]

Molecular biology and TEVC current recordings

The cDNAs (complementary DNAs) for WT human GluN1-1a (hereafter GluN1; GenBank: NP_015566), GluN2A (GenBank: NP_000824), and GluN2B (GenBank: NP_000825) were subcloned in the pCI-neo vector. Site-directed mutagenesis was performed to generate GluN1-M641I using the QuikChange protocol (Stratagene, La Jolla, CA). Preparation of *Xenopus laevis* oocytes, synthesis and injection of cRNA (complementary RNA) into *Xenopus* oocytes were performed as previously described.[18,19] Two-electrode voltage-clamp (TEVC) recordings from *Xenopus* oocytes were performed at room temperature in the recording solution containing (in mmol/L, pH 7.4) 90 NaCl, 1 KCl, 10 HEPES, 0.5 $BaCl_2$, 0.01 EDTA. The membrane potential was held at −40 mV unless stated otherwise.

Concentration–response curves were generated in the presence of maximal glycine (30 μmol/L) and variable glutamate, or maximal glutamate (100 μmol/L) and variable glycine. The agonist concentration–response curves were fitted by the following equation:

$$\text{Response}\,(\%) = 100/\left(1 + (\text{EC}_{50}/[\text{agonist}])^{\text{nH}}\right) \quad (1)$$

where EC_{50} is the agonist concentration that produces a half-maximal response and nH is the Hill slope. The potency of NMDAR channel blockers was determined on the response to maximally effective concentrations of glutamate (100 μmol/L) and glycine (30 μmol/L). IC_{50} values for Mg^{2+} and FDA-approved NMDAR channel blockers were obtained by fitting the concentration–response curves by the following equation:

$$\text{Response}\,(\%) = (100 - \text{minimum})/\left(1 + ([\text{modulator}]/\text{IC}_{50})^{\text{nH}}\right) + \text{minimum} \quad (2)$$

© 2021 The Authors. *Annals of Clinical and Translational Neurology* published by Wiley Periodicals LLC on behalf of American Neurological Association

where IC_{50} is the concentration that produces a half-maximal effect and minimum is the residual inhibition at a saturating concentration of Mg^{2+} or other channel blockers.

The channel open probability (P_{OPEN}) was calculated by measuring the degree of MTSEA (2-aminoethyl methanethiosulfonate hydrobromide; Toronto Research Chemicals, Toronto, Ontario, Canada)[20] potentiation with a cysteine mutation in GluN2A M3 SYTANLAAF gating region (GluN2A-A650C, hereafter A7C), which allows subsequent covalent modification by MTSEA to lock the channels open.[11,21]

$$P_{OPEN} = (\gamma_{MTSEA}/\gamma_{CONTROL}) \times (1/\text{potentiation}) \quad (3)$$

where γ is the channel chord conductance for GluN1/GluN2A before and after MTSEA modification, and potentiation is the ratio of current after 200 μmol/L MTSEA to that observed by 100 μmol/L glutamate and glycine before MTSEA.[11]

Whole-cell voltage-clamp current recordings from mammalian cells

HEK293 cells (ATCC CRL-1573) were transfected using the calcium phosphate method[18] with cDNAs encoding WT GluN1/GluN2A/GFP (1:1:5), WT GluN1/GluN2B/GFP (1:1:1), GluN1-M641I/GluN2A/GFP (1:1:5), or GluN1-M641I/GluN2B/GFP (1:1:1). Following an 18–24 h transfection, whole-cell voltage-clamp current recordings were performed[18,22] at room temperature in recording solution containing (in mmol/L, pH adjusted to 7.4 by addition of NaOH) 150 NaCl, 3 KCl, 10 HEPES, 0.01 EDTA, 0.5 $CaCl_2$, and 11 D-mannitol. The recording electrodes were prepared using borosilicate glass (thin-walled filamented, TW150F-4; WPI, Sarasota, FL) by Narishige P-10 Puller (Tokyo, Japan). The electrodes were filled with an internal solution that contained (in mmol/L) 110 D-gluconic acid, 110 CsOH, 30 CsCl, 5 HEPES, 4 NaCl, 0.5 $CaCl_2$, 2 $MgCl_2$, 5 BAPTA, 2 Na-ATP, 0.3 Na-GTP; the pH was adjusted to 7.35 with CsOH, and the osmolality was adjusted to 300–310 mOsmol kg^{-1} with CsCl or water. The current responses to maximal effectively concentrations of glutamate (1000 μmol/L, in the presence of 100 μmol/L glycine) were recorded using an Axopatch 200B amplifier (Molecular Devices, Sunnyvale, CA) with V_{HOLD} −60 mV, filtered at 8 kHz (−3 dB, 8 pole Bessel filter, Frequency Devices, Ottawa, IL), and digitized at 20 kHz using a Digidata 1440A and Axon Instruments software (Molecular Devices). The deactivation time course following glutamate removal was fitted (ChanneLab, Emory University) with

$$\text{Response} = \text{Amplitude}_{FAST}\exp(-\text{time}/\tau_{FAST}) + \text{Amplitude}_{SLOW}\exp(-\text{time}/\tau_{SLOW}). \quad (4)$$

The weighted deactivation tau (τ_w) was accessed by

$$\tau_w = (\text{Amplitude}_{FAST}\tau_{FAST} + \text{Amplitude}_{SLOW}\tau_{SLOW})/(\text{Amplitude}_{FAST} + \text{Amplitude}_{SLOW}) \quad (5)$$

β-lactamase reporter assay from mammalian cells

For the beta-lactamase (β-lactamase, β-lac) reporter assay, HEK293 cells in 96-well plates were transfected with cDNA encoding WT β-lac-GluN1, β-lac-GluN1-M641I, β-lac-GluN1-M641I/GluN2A, or β-lac-GluN1-M641I/GluN2B using Fugene6 (Promega, Madison, WI).[23] The background absorbance was measured by cells transfected with Fugene6 only. A negative control for surface β-lac activity was determined in cells that were transfected with WT β-lac-GluN1 or β-lac-GluN1-M641I only. Eight wells were transfected for each condition, and the surface and the total β-lac levels were measured in four wells each. The transfected cells were washed with HBSS and 10 mmol/L HEPES after 24-h transfection. The surface activity was measured by adding 100 μL of a 100 μmol/L nitrocefin (Millipore, Burlington, MA) solution in HBSS with HEPES. The total activity was determined by a 30-min incubation in 50 μL H_2O (to lyse the cells) before adding 50 μL of 200 μmol/L nitrocefin. The absorbance was determined by a microplate reader (SpectraMax M2; Molecular Devices) at 468 nm once every min for 30 min (30°C). The rate of the absorbance increase was calculated from the slope of the linear regression.[23]

Evaluation of synaptic and non-synaptic charge transfer

The relative change (in fold) in synaptic and non-synaptic charge transfer was assessed by the following equations.[23]

$$R_{AGONIST} = 1/(1 + (EC_{50}/[\text{agonist}])^{nH}) \quad (6)$$

$$\text{Charge transfer}_{Synaptic} = \tau_{wMUT}/\tau_{wWT} \times P_{MUT}/P_{WT} \times \text{Surf}_{MUT}/\text{Surf}_{WT} \times R_{GLY} \times R_{GLU,\,Synaptic} \times \text{Mg}_{MUT}/\text{Mg}_{WT} \quad (7)$$

$$\text{Charge transfer}_{Non-synaptic} = P_{MUT}/P_{WT} \times \text{Surf}_{MUT}/\text{Surf}_{WT} \times R_{GLY} \times R_{GLU,\,Non-Synaptic} \times \text{Mg}_{MUT}/\text{Mg}_{WT} \quad (8)$$

where [glutamate] is 1×10^{-3} mol/L and 1×10^{-7} mol/L for $R_{GLU,\ Synaptic}$ and $R_{GLU,\ Non\text{-}synaptic}$, respectively,

 © 2021 The Authors. *Annals of Clinical and Translational Neurology* published by Wiley Periodicals LLC on behalf of American Neurological Association

[glycine] is 3×10^{-6} mol/L, and nH is the Hill slope. τ_w is the mean weighted deactivation time constant, P is the channel open probability, Surf is surface protein levels, Mg is percentage inhibition by 1 mmol/L Mg^{2+} at V_{HOLD} −60 mV, and R_{GLY} and R_{GLU} are relative response in a given glutamate or glycine concentration. The τ_w, P, Surf, and Mg for the variants were calculated as a ratio to the WT receptors.

All compounds/agents were purchased from Sigma unless stated otherwise. The number of observations was determined to give a power of 0.8 using GPower (3.1.9.2). All data were presented as mean ± 95% confidence intervals. Statistical significance was established to $p < 0.05$ by unpaired Student's t-test.

RESULTS

Summary of clinical features

The individual is a 24-month-old male born at term to non-consanguineous healthy parents via normal spontaneous vaginal delivery. Birth weight was 6 pounds 15 ounces. Apgar scores were 8 and 9 at 1 and 5 minutes (Table 1). He stayed in the hospital with his mother following the birth and did not have difficulty with feeding or breathing. He was breastfed. At the time of delivery, the mother was found to be group B strep positive and was treated with penicillin; delivery was otherwise uncomplicated. The parents first noticed "startles" during the first 1 to 2 weeks of life, during which the patient extended his arms suddenly, with each episode lasting 1 to 2 sec. The episodes occurred at least 10 times daily, did not increase in frequency or severity, and lasted until the patient was 10 weeks of age. At 12 weeks of age, the patient developed episodes of brief head turning to the right side with rapid side-to-side eye movements, accompanied by bilateral arm extension and leg flexion, occurring multiple times per day, lasting only seconds each time. These episodes increased in severity and frequency, becoming too numerous to count.

The patient was initially admitted to a children's hospital at 4 months of age where long-term video EEG monitoring was performed, showing evidence of infantile spasms and tonic seizures. In addition, the EEG background activity was characterized by bursts of high amplitude interictal epileptiform discharges alternating with brief epochs of electrocerebral suppression lasting 4 to 5 sec, deemed consistent with an early infantile epileptic encephalopathy syndrome. MRI brain was normal at 3 months of age (Fig. 1). The patient was treated with ACTH (150 Unit/m^2). With ACTH treatment, the epileptic spasms were less severe and demonstrated a 50% reduction in frequency without complete resolution, as reported by the patient's family and confirmed with long-term video EEG monitoring. As the ACTH taper was undertaken within 4 weeks, the spasms worsened to near pretreatment levels at 30–50 times a day. Repeat long-term video EEG monitoring showed generalized bursts of

Table 1. The patients' and the variant's information.

	Patient-1	Patient-2
Gender	Male	Male
Age	24 months	14 years
Diagnosis	EOEE	EOEE
Family history	Normal	Normal
Perinatal period	The mother was found to be group B strep positive	NA
Age at onset	2 months	2 months
Seizure types	Epileptic spasms started at 2 months and developed tonic-clonic seizures after 12 months of age	Breath-holding attack, abnormal eye movement with tonic posture unilateral limb
EEG features	Infantile spasms, tonic seizures	Diffuse spike-wave and polyspike-wave bursts at 3 months, focal spike or spike-waves in the bilateral frontopolar area at 13 years
Response to medication	Transient response to ACTH, then the spasms recurred; no response to VIG, FBM, CLB	Refractory to VPA, CBZ, PB
Developmental delay	Severe	Severe
Hypotonia and movement disorder	Hypotonia with poor head control, appendicular hypertonia and spasticity, and diffuse hyperreflexia	Stereotyped movements of fingers; peculiar involuntary movements groaning with head swaying and breath held
MRI	Normal	Cerebral atrophy
Other neurological features	Difficulty to arouse, drowsy	Laughs without reason, no purposeful hand skills
Source	This study	Ohba et al[10]
GRIN1 variant		
cDNA (NM_000832)	c.1923G>A	c1923G>A
Protein	p.Met641Ile	p.Met641Ile
Inheritance	de novo	de novo
Location	M3	M3

ACTH, adrenocorticotropic hormone; CBZ, carbamazepine; CLB, clobazam; EOEE, early-onset epileptic encephalopathies; FBM, felbamate; PB, phenobarbital; VIG, vigabatrin; VPA, valproic acid.

© 2021 The Authors. *Annals of Clinical and Translational Neurology* published by Wiley Periodicals LLC on behalf of American Neurological Association

very high amplitude interictal epileptiform discharges, intermittently alternating with epochs of electrical cerebral suppression. Felbamate was started at 10 mg/kg per day and rapidly titrated up to 100 mg/kg per day. Clobazam (2.5 mg) was also added in the evening to help with sleep initiation and continued seizures. Vigabatrin (175 mg/kg per day) was subsequently added to the regimen of high dose felbamate and low dose clobazam. The patient continued to have refractory epileptic spasms and tonic seizures, up to 30–50 times a day (Table 1). After 10 months of age, the patient also developed tonic-clonic seizures, two to three times a day lasting for 30–60 sec.

Upon initial physical examination at 12 months of age, the patient was encephalopathic. He had no eye contact and was not tracking visually. He had axial hypotonia with poor head control, appendicular hypertonia and spasticity, and diffuse hyperreflexia. Ophthalmological examination was unremarkable. Subsequent examination at 24 months demonstrated intermittent random arm and hand chorea movements, with minimal eye contact, spasticity in all extremities, and diffuse hyperreflexia.

Whole-exome sequencing result and pathogenicity prediction

Whole-exome sequencing performed at 6 months of age, identified a de novo heterozygous missense variant (c.1923G>A, p.Met641Ile) in exon 13 of the *GRIN1* gene. This variation produced a methionine to isoleucine substitution in the M3 transmembrane helix of GluN1

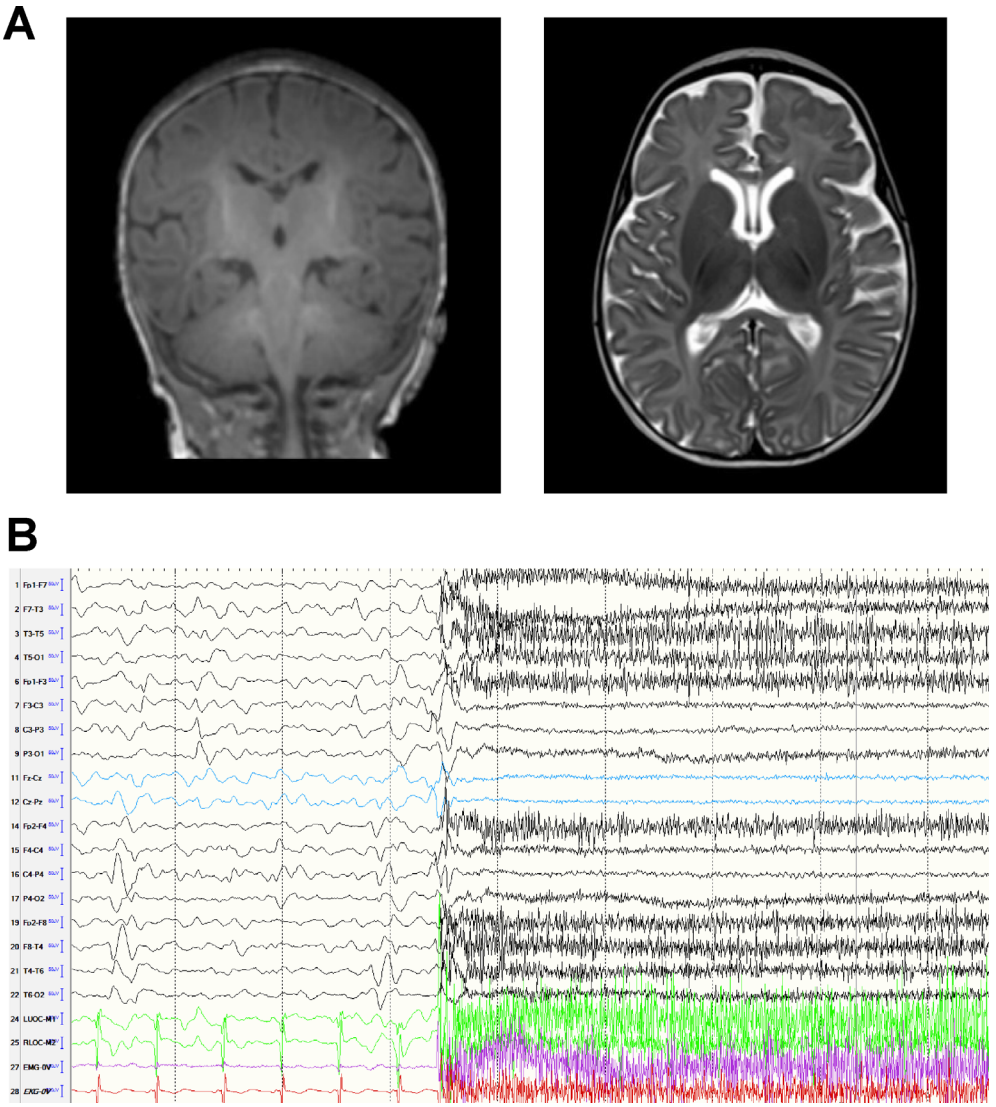

Figure 1. Brain MRI and EEG features of the patient with the M641I variant. (A) MRI of the brain at 3 months of age was normal. (B) Ictal EEG at 9 months of age showed electro decrement superimposed with fast activity and myogenic artifacts in a patient with typical epileptic spasms.

 © 2021 The Authors. *Annals of Clinical and Translational Neurology* published by Wiley Periodicals LLC on behalf of American Neurological Association

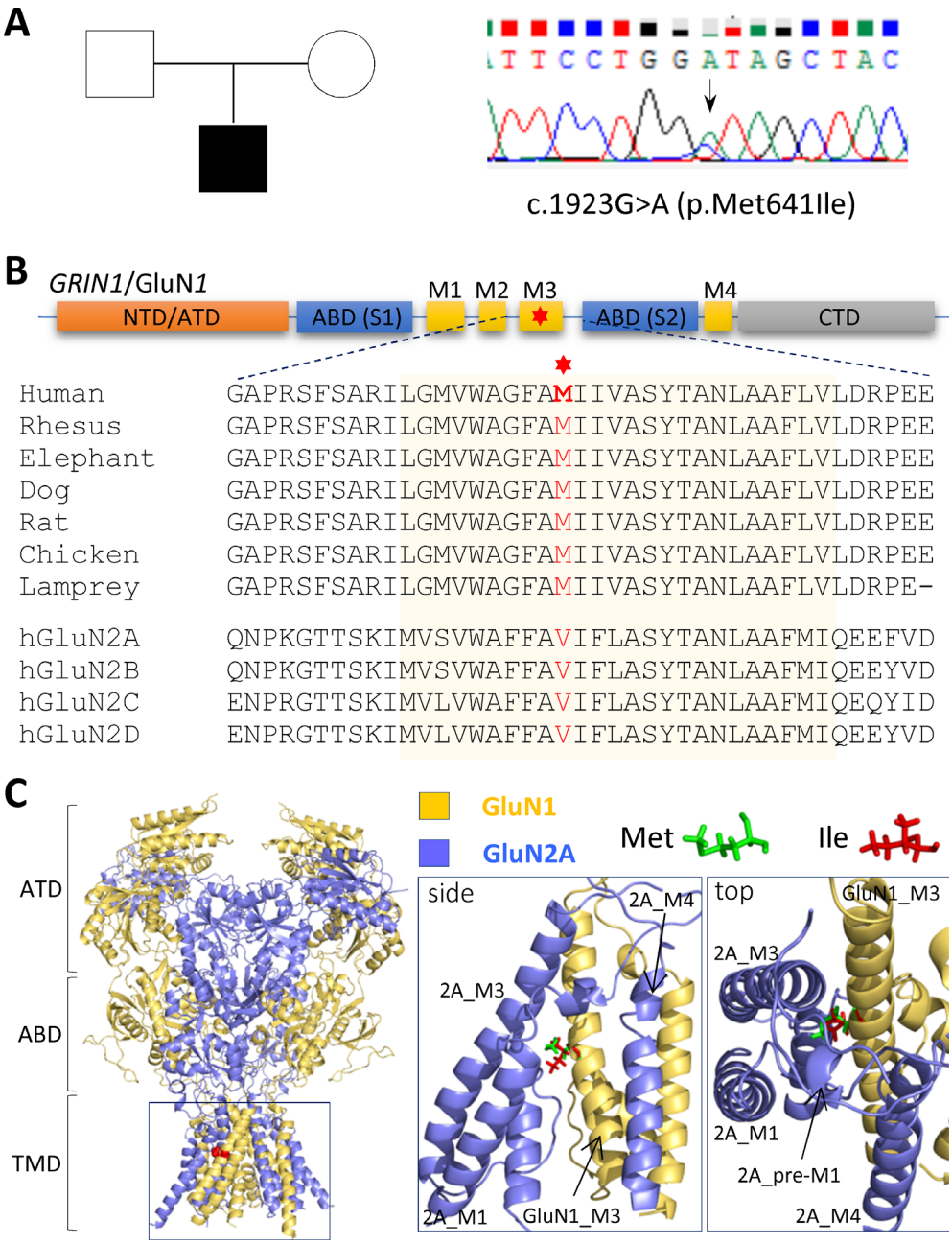

Figure 2. De novo *GRIN1* c.1923G>A (GluN1 p.Met641Ile) variant. (A) A de novo *GRIN1* missense variant (c.1923G>A, p.Met641Ile) was identified in a male patient using the next-generation whole-exome sequencing. (B) A linear schematic representation of the GluN1 subunit (the position of M641 is marked with red). The Methionine residue at position 641 is highly conserved across most of the subphylum *Vertebrata*. (C) A homology model of GluN1/GluN2A subunit built from the GluN1/GluN2B crystallographic data.[34,35] The GluN1-M641I residue resides in the M3 transmembrane helix. The substitution of an amino acid (methionine to isoleucine) is shown as a stick model and marked with a different color.

(Fig. 2). Notably, this methionine is highly conserved across the *GRIN1* gene in most vertebrata species (Fig. 2 B), but not in the GluN2 subunits encoded by *GRIN2A-D* genes. This variant has not been previously reported in the healthy population (gnomAD database, evaluated on 09 December 2020). We evaluated the pathogenicity prediction according to the ACMG guideline 2015[17] and the results indicate this variant as "likely pathogenic" (Table 1). This variant was previously described in a patient,[10] and another pediatric epilepsy patient harboring this variant has recently been identified (M. Kruer, personal communication).

© 2021 The Authors. *Annals of Clinical and Translational Neurology* published by Wiley Periodicals LLC on behalf of American Neurological Association

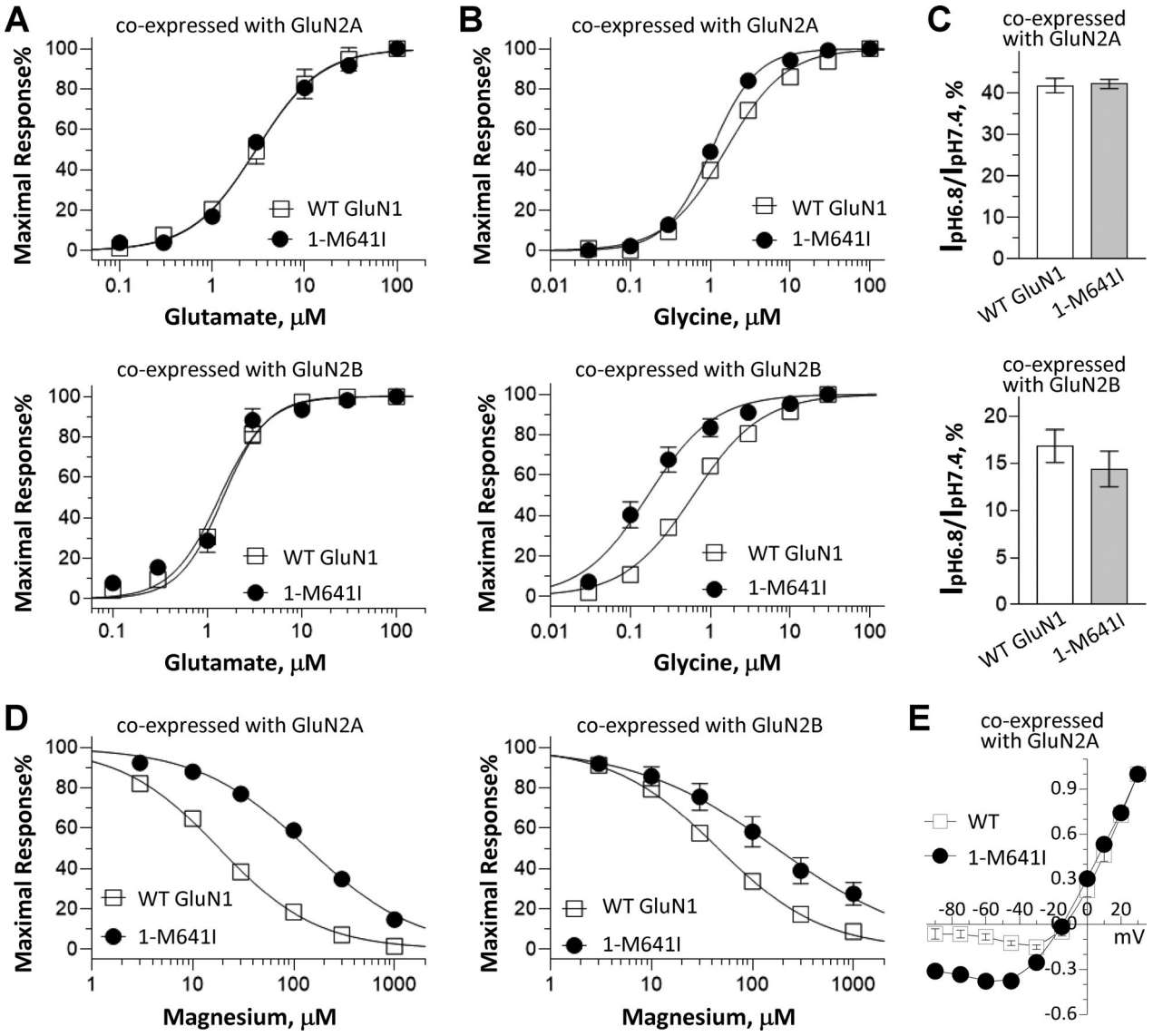

Figure 3. GluN1-M641I alters NMDAR pharmacological properties. (A and B) Composite concentration–response curves for glutamate (A, in the presence of 100 μmol/L glycine) and glycine (B, in the presence of 100 μmol/L glutamate) recorded at a holding potential of −40 mV for WT GluN1 and GluN1-M641I co-expressed with GluN2A (*upper panels*) or GluN2B (*lower panels*), respectively. (C) Summary of proton sensitivity evaluated by current ratio at pH 6.8 to pH 7.6 (in the presence of 100 μmol/L glutamate and 100 μmol/L glycine) at a holding potential of −40 mV of the WT GluN1 and GluN1-M641I when co-expressed with GluN2A (*upper panel*) and GluN2B (*lower panel*), respectively. (D) Composite concentration–response curves for Mg^{2+} in the presence of 100 μmol/L glutamate and 100 μmol/L glycine at a holding potential of −60 mV of the WT GluN1 and GluN1-M641I when co-expressed with GluN2A (*left panel*) and GluN2B (*right panel*), respectively. (E) Mg^{2+} current–voltage (*I–V*) curves for the WT GluN1 and GluN1-M641I co-expressed with GluN2A. All current responses were normalized to the current recorded at +30 mV. Composite data are shown as mean ± SEM. NMDAR, N-methyl-D-aspartate receptor; WT, wild-type.

GluN1-M641I alters NMDAR pharmacological properties

We first investigated the influence of the variant on receptor pharmacological properties using the *Xenopus* oocyte expression system and TEVC recordings. Agonist potency was determined by measuring the response to a range of glutamate or glycine concentrations. GluN1-M641I-containing NMDARs had a glutamate potency similar to WT GluN1, with glutamate EC_{50} values for GluN1/GluN2A of 3.8 μmol/L (M641I) versus 3.4 μmol/L (WT) and glutamate EC_{50} values for GluN1/GluN2B of 1.5 μmol/L (M641I) versus 1.5 μmol/L (WT) (Fig. 3A, Table 2). NMDARs that contained the GluN1 variant

 © 2021 The Authors. *Annals of Clinical and Translational Neurology* published by Wiley Periodicals LLC on behalf of American Neurological Association

Table 2. Summary of the functional effects and rescue pharmacology.

	Co-expressed with GluN2A		Co-expressed with GluN2B	
	WT GluN1	GluN1-M641I	WT GluN1	GluN1-M641I
Glutamate EC_{50}, μmol/L (*n*)	3.8 (2.6, 5.0) (10)	3.4 (2.6, 4.2) (15)	1.5 (1.3, 1.8) (9)	1.5 (1.0, 2.1) (11)
Glycine EC_{50}, μmol/L (*n*)	1.9 (1.3, 2.4) (13)	1.1 (1.0, 1.2) (19)*	0. 68 (0.52, 0.84) (11)	0.27 (0.14, 0.41) (13)*
%, $pH_{6.8}/pH_{7.6}$[a]	42 (38, 45) (13)	42 (40, 44) (12)	17 (13, 20) (10)	14 (11, 18) (13)
Mg IC_{50}, μmol/L (*n*)[b]	20 (16, 23) (17)	161 (118, 204) (19)*	46 (33, 59) (13)	408 (222, 594) (15)*
% inhibition at 1 mmol/L Mg[b,c]	98 (97, 100) (17)	85 (80, 90) (19)*	91 (89, 94) (13)	72 (61, 84) (15)*
Mg IV, % at −60mV (*n*)[d]	8.4 (3.0, 12) (6)	38 (30, 42) (6)*	–	–
P_{OPEN}, MTSEA	0.26 (0.21, 0.31) (6)	0.09 (0.08, 0.10) (8)*	–	–
Amplitude, pA/pF	137 (32, 242) (5)	73 (30, 115) (6)	–	–
Deactivation τ_w, ms	54 (44, 63) (5)	65 (52, 78) (6)	–	–
Surface/total ratio (beta-lac)	1.0 (5)	0.71 (0.52, 0.90) (5)*	1.0 (6)	1.1 (0.83, 1.3) (6)
Synaptic charge transfer[e]	1.0	3.6	–	–
Non-synaptic charge transfer[e]	1.0	2.2	–	–
Memantine IC_{50}, μmol/L (%, *n*)[f]	4.4 (3.5, 5.3) (93%, 18)	1.3 (0.92, 1.6) (97%, 23)*	3.0 (2.0, 4.1) (97%, 9)	0.84 (0.67, 1.0) (99%, 16)*
Ketamine IC_{50}, μmol/L (%, *n*)[f]	7.8 (5.2, 10) (91%; 12)	0.93 (0.86, 1.0) (95%, 8)*	4.3 (2.8, 5.7) (91%, 13)	0.63 (0.23, 1.0) (93%, 16)*
Dextromethorphan IC_{50}, μmol/L (%, *n*)[f]	8.5 (5.6, 11) (93%; 7)	0.42 (0.33, 0.52) (95%, 9)*	9.1 (5.3, 13) (95%, 6)	1.2 (0.77, 1.7) (93%, 12)*
Dextrorphan IC_{50}, μmol/L (%, *n*)[f]	1.1 (0.61, 1.6) (94%; 7)	0.08 (0.06, 0.10) (98%, 10)*	0.28 (0.18, 0.37) (98%, 7)	0.06 (0.05, 0.07) (98%, 6)*
Amantadine IC_{50}, μmol/L (%, *n*)[f]	157 (110, 203) (87%; 6)	14 (11, 17) (97%, 14)*	48 (36, 59) (95%, 6)	7.3 (5.1, 9.6) (99%, 7)*
TCN-201 IC_{50}, μmol/L (%, *n*)[f,g]	0.20 (0.17, 0.22) (97%, 7)	0.22 (0.18, 0.26) (99%, 7)	–	–

The data are expressed as mean (−95% CI, +95% CI) (*n*). CI, confidence intervals; WT, wild-type.

[a]Percentage of the current recorded at pH 6.8 as a ratio to that recorded at pH 7.6.

[b]Recorded at −60 mV holding potential.

[c]Percentage current remaining in the presence of 1 mmol/L Mg^{2+} compared to the agonist-evoked current (100 μmol/L glutamate and glycine) the nominal absence of Mg^{2+}.

[d]Percentage current recorded at −60 mV normalized to the current recorded at +30 mV.

[e]The values of predicted synaptic and non-synaptic changes of the M641I variant relative to the WT receptor (set as 1.0) were calculated by Equations 6–8, and provide the fold difference in synaptic and non-synaptic receptor function.

[f]Data are ratio of current in drug to current in the absence of drug, presented as mean (−95% CI, +95% CI) (max inhibition %, *n*); max inhibition % at 100 μmol/L memantine, 100 μmol/L ketamine, 300 μmol/L dextromethorphan, 30 μmol/L dextrorphan, 1000 μmol/L amantadine, and 10 μmol/L TCN-201.

[g]In the presence of 100 μmol/L glutamate and 3 μmol/L glycine.

*$p < 0.05$ $LogEC_{50}$ or $LogIC_{50}$, *p* value was determined by unpaired *t*-test comparing with the WT GluN1 co-expressed with WT GluN2A or WT GluN2B; controlled FWER (family wise error rate) by using the Holm–Bonferroni correction if multiple parameters were compared from the same recordings, and also presented when the 95% confidence intervals of the experimental datasets do not overlap.

showed a modest, but significant, increase in glycine potency, with an EC_{50} for GluN1/GluN2A of 1.1 μmol/L (M641I) versus 1.8 μmol/L (WT) and an EC_{50} for GluN1/GluN2B of 0.27 μmol/L (M641I) versus 0.68 μmol/L (WT) (Fig. 3B, Table 2).

We subsequently evaluated the effects of the variant on the sensitivity of endogenous negative modulators. The GluN1-M641I variant presents no significant difference in proton sensitivity when co-expressed with GluN2A or GluN2B (Fig. 3C, Table 2). Remarkably, the GluN1-M641I variant showed an 8- to 9-fold decrease in Mg^{2+} potency, with IC_{50} values for GluN1/GluN2A increased to 161 μmol/L (M641I) from 20 μmol/L (WT), and IC_{50} values for GluN1/GluN2B increased to 408 μmol/L (M641I) from 46 μmol/L (WT). There was also a significant decrease in maximum percentage

© 2021 The Authors. *Annals of Clinical and Translational Neurology* published by Wiley Periodicals LLC on behalf of American Neurological Association

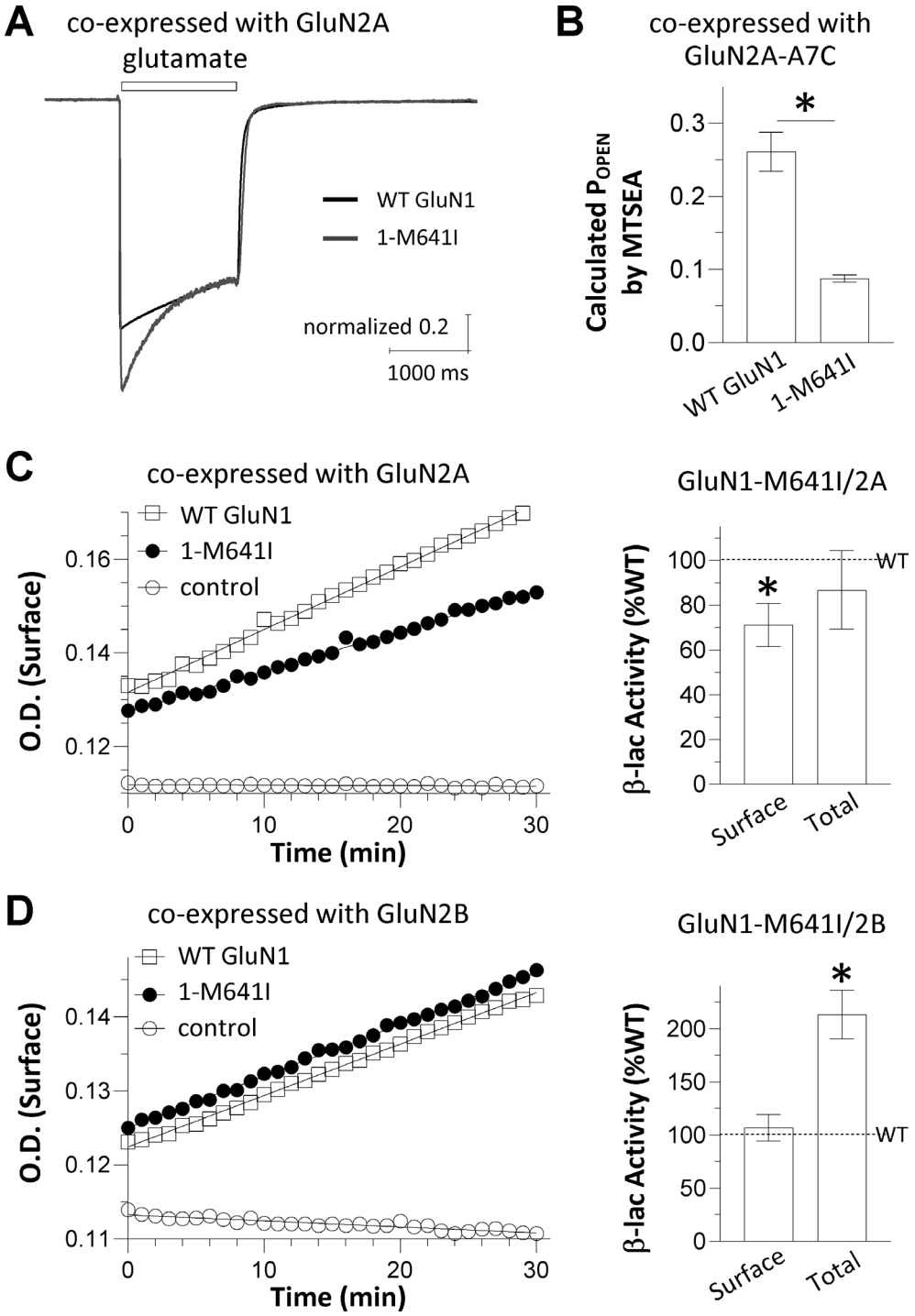

Figure 4. GluN1-M641I alters NMDAR open probability and surface expression. (A) Representative recordings of the current response time course obtained from whole-cell voltage-clamp recordings of HEK cells transfected with the WT GluN1/GluN2A (*Black*) and GluN1-M641I/GluN2A (*Gray*) at a holding potential of −60 mV in response to rapid application of 1000 μmol/L glutamate in the presence of 100 μmol/L glycine. (B) The channel open probability was assessed by measuring the degree of MTSEA (0.2 mmol/L) potentiation using TEVC recordings from *Xenopus* oocytes expressing the WT GluN1 or GluN1-M641I coexpressed with GluN2A-A650C (hereafter 2A-A7C) in the presence of 100 μmol/L glutamate and glycine at a holding potential of −40 mV. (C and D) Representative plots of nitrocefin absorbance (optical density, O.D.) versus time course are indicated for HEK cells transfected with the WT β-lac-GluN1 and β-lac-GluN1-M641I when co-expressed with GluN2A (C) and GluN2B (D), respectively. The slopes of O.D. versus time were averaged as percentages of the WT NMDAR for the ratio of surface/total from five to six independent experiments. Data are presented as mean ± SEM, and were analyzed by unpaired *t*-test (*$p < 0.05$, compared to WT). NMDAR, N-methyl-D-aspartate receptor; WT, wild-type.

 © 2021 The Authors. *Annals of Clinical and Translational Neurology* published by Wiley Periodicals LLC on behalf of American Neurological Association

inhibition at 1 mmol/L Mg^{2+} (Fig. 3D, Table 2). In addition, the current–voltage (*I–V*) curves indicated 4.5-fold more current (relative current at −60 mV normalized to the current at +30 mV) (Fig. 3E, Table 2) in the variant when co-expressed with GluN2A. These results suggest that the GluN1-M641I significantly reduced the voltage-dependent Mg^{2+} inhibition.

GluN1-M641I alters receptor biophysical properties and receptor trafficking

To assess the effect of GluN1-M641I on the deactivation rate, we recorded current responses to prolonged application of glutamate (1.5 sec) under whole-cell voltage clamp from transfected HEK cells to measure the current response time course following glutamate removal. GluN1-M641I showed a comparable glutamate deactivation time course when co-expressed with GluN2A (weighted tau, τ_w 65 ms for M641I vs. 54 ms for WT; Fig. 4A, Table 2). These data suggest that the GluN1-M641I variant has little effect on the deactivation response time course, and likely does not alter the time course of synaptic currents. We then assessed the effect of the GluN1-M641I variant on channel open probability by measuring the degree of MTSEA potentiation of the NMDAR response to maximally effective glutamate and glycine (100 μmol/L) in TEVC recordings on *Xenopus* oocytes. The current increase induced by MTSEA is reciprocally related to the channel open probability prior to the MTSEA application. Our data indicated that channel open probability for GluN1-M641I/GluN2A decreased by 2.9-fold, and was 0.09 for M641I versus 0.26 for WT (Fig. 4B, Table 2), suggesting the variant reduces channel open probability.

To investigate whether the GluN1-M641I variant influences NMDA receptor surface expression, we used a β-lactamase reporter assay in HEK cells to quantify the level of cell surface GluN1 and total GluN1 protein. Co-expression of GluN1-M641I/GluN2A showed a significant reduction in the ratio of surface-to-total GluN1 protein level compared to WT (71% of WT, Fig. 4C, Table 2, Tables S1 and S3), whereas co-expression of GluN1-M641I/GluN2B produced a comparable ratio of surface-to-total GluN1 protein compared to WT NMDARs (107% of WT, Fig. 4D, Table 2, Tables S2 and S3). These data suggest that the GluN1-M641I variant produces a significant reduction in surface expression of GluN1 when co-expressed with GluN2A in heterologous expression systems.

Evaluating the net impact of GluN1-M641I on NMDAR function

The functional changes caused by the GluN1-M641I variant coexpressed with GluN2A are somewhat conflicting. Some changes should increase current responses (i.e., increased agonist potency, reduced Mg^{2+} inhibition), whereas others should decrease current responses (i.e., decreased P_{OPEN}, reduced surface expression). We employed a strategy to estimate the functional consequence of all measured changes produced by this variant on synaptic and non-synaptic charge transfer for comparison to WT NMDARs. This approach can provide a first approximation of the net effect of the variant on neuronal NMDAR function by combining measurements of multiple parameters.[23] This calculation revealed that the GluN1-M641I variant should enhance synaptic and non-synaptic charge transfer by 3.6- and 2.2-fold, respectively (Table 2, Table S4), and suggested that functional enhancements resulted by decreased Mg^{2+} block more than offset the moderately reduced surface expression and decreased open probability. Therefore, the net effect of these changes suggests that GluN1-M641I is overall a gain-of-function variant.

GluN1-M641I is more sensitive to FDA-approved NMDARs channel blockers

Since the patient's seizures were resistant to anti-seizure drugs, a set of FDA-approved NMDAR blockers was assessed for their ability to inhibit recombinant NMDARs that contained GluN1-M641I. We performed TEVC recordings on *Xenopus* oocytes to determine the IC_{50} value for NMDAR channel blockers including amantadine, memantine, ketamine, dextromethorphan, and the dextromethorphan metabolite dextrorphan. The results revealed that all FDA-approved drugs evaluated showed enhanced potency (i.e., decreased IC_{50} values) on the GluN1-M641I-containing NMDARs by 3.4- to 20-fold (Fig. 5A–E, Table 2) in comparison to the WT receptors. These data raise the possibility that the GluN1-M641I variant is more sensitive to these organic cationic channel blockers. In contrast, TCN-201, a GluN2A-selective negative allosteric modulator showed a comparable potency between the WT and GluN1-M641I variant (Fig. 5F, Table 2), which is consistent with the effects of the variant of mild change in glycine potency.

Personalized therapy with memantine

Memantine was added as an adjunct treatment to the patient's antiepileptic drug regimen (Vigabatrin 175 mg/kg per day, Felbamate 100 mg/kg per day, Clobazam 2.5 mg/kg per day) at 14 months of age, started at 0.2 mg/kg per day, and slowly increased to 0.4 mg/kg per day in 2 weeks. Three weeks later, the spasms and tonic seizures decreased significantly in frequency and severity, from 20 to 30 times a day to a few times a day (by parent diary; Fig. 6A). After 3 months of treatment, the spasms dropped to once every 2–3 weeks (Fig. 6A).

© 2021 The Authors. *Annals of Clinical and Translational Neurology* published by Wiley Periodicals LLC on behalf of American Neurological Association

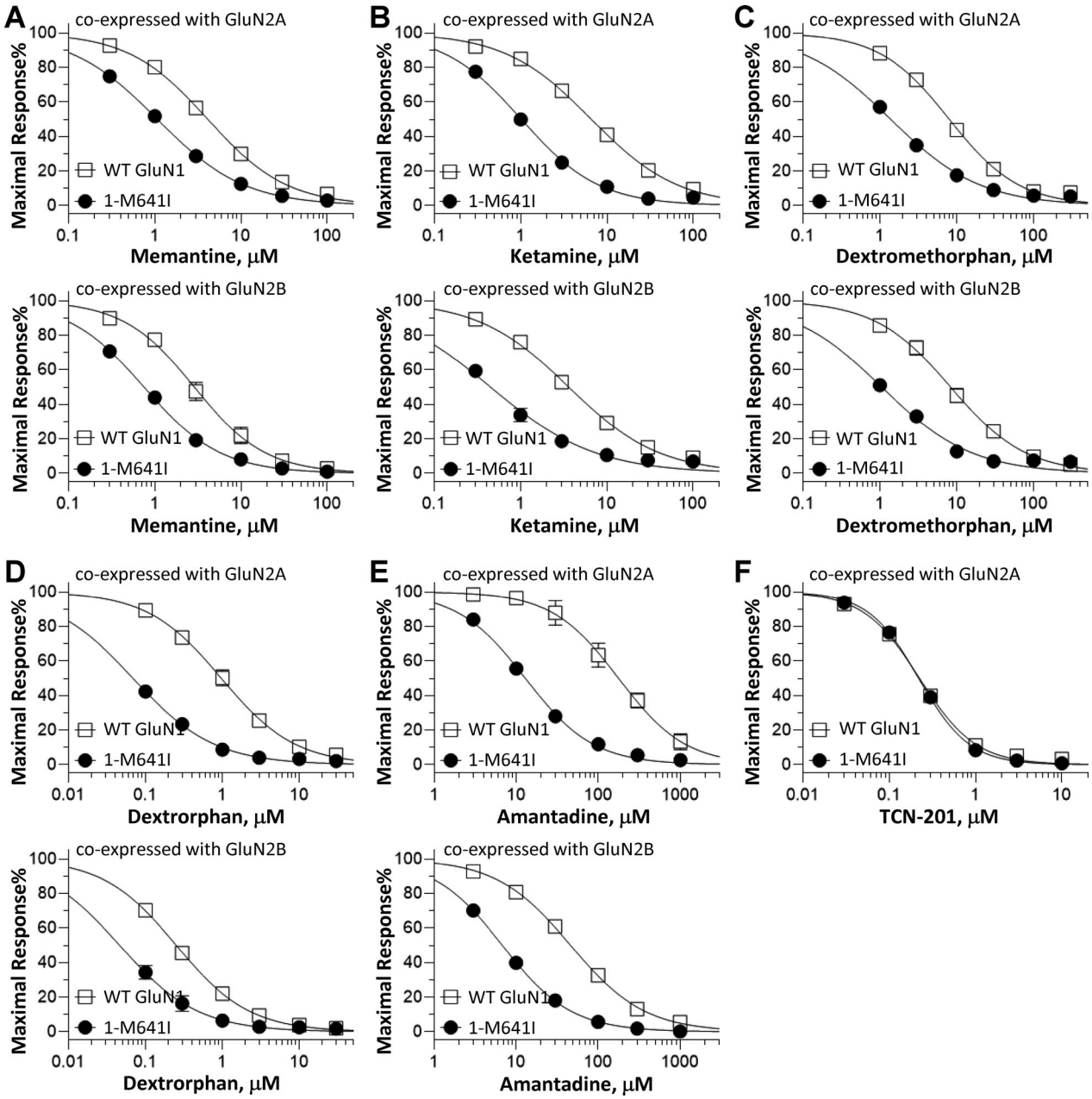

Figure 5. The effect of NMDAR antagonists, including FDA-approved drugs, on the WT and GluN1-M641I NMDARs. Composite concentration–response curves of NMDAR antagonists were evaluated by TEVC recordings of *Xenopus* oocytes in the presence of 100 μmol/L glutamate and 100 μmol/L glycine (except for TCN-201 with 3 μmol/L glycine) at a holding potential of −40 mV. Curves are shown for (A) memantine, (B) ketamine, (C) dextromethorphan, (D) memantine, (E) amantadine, and (F) TCN-201. Data are shown as mean ± SEM; SEM is shown when larger than symbol size. NMDAR, N-methyl-D-aspartate receptor; TEVC, two-electrode voltage-clamp; WT, wild-type.

Repeat EEG after 3 months of treatment demonstrated mild abnormalities with subtle background slowing and no interictal epileptiform discharge (Fig. 6B). In addition, the patient was more alert and calmer by parental reports. His sleep also improved significantly on Clonidine. His seizure frequency remained unchanged, at one spasm every 2–3 weeks. At 17 months of age, the patient missed three doses of memantine with concurrent brief recurrence of spasms and tonic-clonic seizures, with spasms occurring five to seven times per day. Two days after restarting memantine, the tonic-clonic seizures stopped and the spasms became far less frequent, occurring only a few times per day (Fig. 6A). Six months after memantine was restarted, the seizures remained under

 © 2021 The Authors. *Annals of Clinical and Translational Neurology* published by Wiley Periodicals LLC on behalf of American Neurological Association

A **Seizure Frequency before and after memantine treatment**

	epileptic spasms	tonic-clonic seizures
before memantine	150-200/week	10-20/week
3 months after memantine	1-2 /week	0-2/week
2 days after discontinuation	30-50/week	15-20/week
1 week after restart	10-20/week	5-10/week
6 months after restart	7-14/week	3-5/week

B

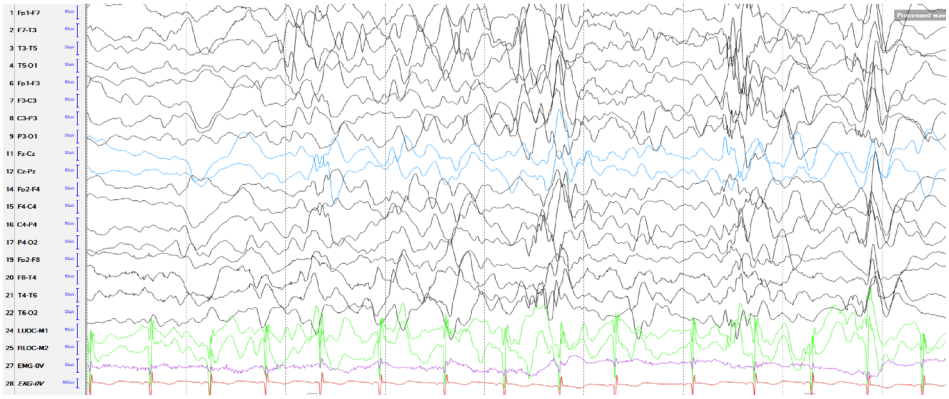

C

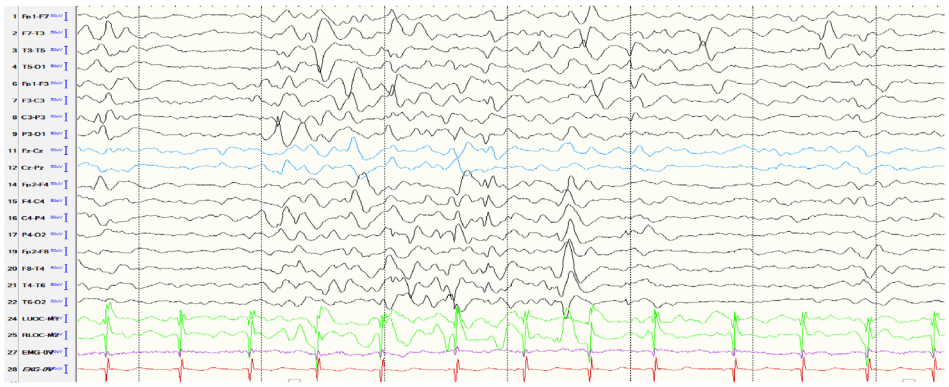

D

Figure 6. The effect of memantine on patient's seizure frequency and EEG. (A) Addition of memantine to the anticonvulsant regimen reduced the seizure frequency significantly; the patient was also on Felbamate, Vigabatrin and Clobazam. Seizure frequency was determined by a parental observation log. The patient accidentally missed 2 days of memantine after 3 months of treatment, over which time the seizures increased significantly. One week after restarting memantine, the seizure frequency dropped significantly again. Six months after the memantine treatment, the seizures were still under good control. (B–D) Routine EEG before and after memantine treatment. Before the treatment at 4 months of age (B), the EEG showed hypsarrhythmia pattern and moderate slow background and abundant multifocal epileptiform discharges at 9 months of age (C) However, after the treatment at 18 months of age (D), the EEG only showed mild slow EEG background without epileptiform discharge.

© 2021 The Authors. *Annals of Clinical and Translational Neurology* published by Wiley Periodicals LLC on behalf of American Neurological Association

good control, 10–20 times a week. At his most recent follow-up appointment, he was taking memantine 0.5 mg/kg per day, vigabatrin 90 mg/kg per day, and felbamate 70 mg/kg per day. No side effects were reported by his parents.

DISCUSSION

Genetic variations in *GRIN1* genes have been identified in certain neurological and neuropsychiatric disorders, including intellectual disability and epilepsy syndromes. In this study, we reported a recurrent de novo missense variant *GRIN1 c*.1923G>A which results in a p.Met641Ile substitution in a patient (Patient-1) with infantile spasms. This variant was also identified previously in a male patient (Patient-2).[10] Both patients were diagnosed as early-onset epileptic encephalopathy with seizure onset at 2 months of age and medically refractory epilepsy. Both patients presented similar clinical features such as severe developmental delay and movement disorders. A third patient with this variant has also been reported (M. Kruer, personal communication), who shares a similar phenotype. The patient described here had no clear abnormalities on his brain MRI at 3 months of age, while the brain MRI for Patient-2 indicated cerebellar atrophy (Table 1).

The methionine residue at position 641 is located in the M3 transmembrane helix (Fig. 2C), which forms a helical bundle crossing that physically occludes the channel pore and must change its position to let ions pass through, therefore playing a particularly key role in channel gating.[1,24,25] In this study, we provided the first comprehensive evaluation of the effects of the GluN1-M641I on the receptor's pharmacological and biophysical properties, as well as surface trafficking. The functional data described here with recombinant NMDARs consisted of GluN1-M641I and WT GluN2A or GluN2B revealed that the variant influences the receptor function by multiple aspects and has conflicting consequences. Enhanced agonist (glycine) potency and reduced Mg^{2+} inhibition appear to increase receptor function, whereas decreased channel open probability and reduced surface expression may decrease receptor function. This further emphasizes the necessity of comprehensive evaluation on the overall impact of *GRIN* variant on receptor function to avoid misleading conclusions caused by evaluating only one aspect of receptor function.[16] We used an approach that combines the variant's multiple effects on NMDAR pharmacological, intrinsic biophysical properties, and surface expression to provide a quantitative prediction of the overall impact of the variant.[16,23] This analysis suggested that the GluN1-M641I variant contributes to an enhanced NMDAR synaptic and nonsynaptic signaling. Taken together, the functional alteration caused by the variant is likely underlying the patients' phenotype.

To determine whether available compounds can mitigate the variant's altered enhanced function, several low-affinity FDA-approved NMDAR channel blockers were evaluated. Our data indicate that the GluN1-M641I variant is significantly more sensitive than the WT receptors to all five channel blockers (memantine, ketamine, dextromethorphan/dextrorphan, and amantadine) evaluated, which is in contrast to most gain-of-function *GRIN* variants assessed previously with differential sensitivity to distinct blockers.[8,18,19,22,23,26-29] The data suggest that these drugs have the potential to alleviate the variant-induced NMDA receptor overactivation and mitigate excitotoxicity. Some of these blockers (i.e., memantine) have been suggested to be safe in pediatric patients,[30,31] raising the possibility that these drugs might be clinically useful as pharmacological approaches.

"N of 1" compassionate use trials have been applied in several pediatric patients hosting gain-of-function *GRIN2A, GRIN2B, or GRIN2D* variants with drug-resistant seizures and early-onset epileptic encephalopathy and showed a divergent response to off-label use of memantine.[8,16,19,26,28,32,33] Our patient responded favorably to memantine with a significant decrease in frequency and severity of spasms and tonic seizures. When the patient accidentally missed three doses of memantine, his seizures/spasms recurred. After restarting memantine, the seizures/spasms dramatically improved, further demonstrating memantine's effectiveness for his epilepsy. At his last follow-up appointment, the patient had been on memantine for over 9 months, and his seizures remained under good control despite lowering the doses of his antiepileptic medications. The favorable clinical response to memantine may reflect the fact that this variant has enhanced the potency of this compound at the variant receptor.

In summary, we reported a patient with a recurrent pathogenic *GRIN1* c.1923G>A variant, performed a comprehensive in vitro functional evaluation of the variant, and assessed the effects of a set of FDA-approved NMDAR channel blockers in an attempt to mitigate the altered function caused by the variant. An "N of 1" memantine trial significantly improved the patient's seizure burden, with evidence of efficacy when seizures worsened considerably during transient discontinuation of memantine. Our findings contribute to further understanding for phenotype–genotype correlations of patients with *GRIN* gene variants and provide potential guidance for the future use of precision medicine. Appropriate clinical trials including more *GRIN1* patients are necessary to further establish the safety and efficacy, especially with respect to neurodevelopmental outcomes, for long-term

 © 2021 The Authors. *Annals of Clinical and Translational Neurology* published by Wiley Periodicals LLC on behalf of American Neurological Association

use memantine in stratified individuals with GRIN gain-of-function variants.

Acknowledgments

The authors thank Jing Zhang, Phoung Le, Chun Hu, and Hirofumi Kusumoto for technical support. The authors also thank Drs. Tim Benke, Annapurna Poduri, and Michael Kruer for their critical reading of the manuscript.

Conflicts of Interest

Nothing of direct relevance to the current research to report.

Authors' Contributions

S.F.T., G.Z., and H.Y. contributed to the conception and design of the study. G.Z., D.S., and S.G. contributed to phenotyping and collecting clinical information. Y.X., R.S., W.C., and K.L.S. performed the experiments. Y.X., R.S., W.C., K.L.S., S.F.T., and H.Y. contributed to the analysis of data. All authors contributed to the manuscript preparation.

REFERENCES

1. Traynelis SF, Wollmuth LP, McBain CJ, et al. Glutamate receptor ion channels: structure, regulation, and function. Pharmacol Rev 2010;62:405–496.
2. Hansen KB, Wollmuth LP, Bowie D, et al. Structure, function, and pharmacology of glutamate receptor ion channels. Pharmacol Rev 2021;73.
3. Akazawa C, Shigemoto R, Bessho Y, et al. Differential expression of five N-methyl-D-aspartate receptor subunit mRNAs in the cerebellum of developing and adult rats. J Comp Neurol 1994;347:150–160.
4. Paoletti P, Bellone C, Zhou Q. NMDA receptor subunit diversity: impact on receptor properties, synaptic plasticity and disease. Nat Rev Neurosci 2013;14:383–400.
5. Yuste R, Majewska A, Cash SS, Denk W. Mechanisms of calcium influx into hippocampal spines: heterogeneity among spines, coincidence detection by NMDA receptors, and optical quantal analysis. J Neurosci 1999;19:1976–1987.
6. Hansen KB, Yi F, Perszyk RE, et al. Structure, function, and allosteric modulation of NMDA receptors. J Gen Physiol 2018;150:1081–1105.
7. Lau CG, Zukin RS. NMDA receptor trafficking in synaptic plasticity and neuropsychiatric disorders. Nat Rev Neurosci 2007;8:413–426.
8. Pierson TM, Yuan H, Marsh ED, et al. GRIN2A mutation and early-onset epileptic encephalopathy: personalized therapy with memantine. Ann Clin Transl Neurol 2014;1:190–198.
9. Burnashev N, Szepetowski P. NMDA receptor subunit mutations in neurodevelopmental disorders. Curr Opin Pharmacol 2015;20:73–82.
10. Ohba C, Shiina M, Tohyama J, et al. GRIN1 mutations cause encephalopathy with infantile-onset epilepsy, and hyperkinetic and stereotyped movement disorders. Epilepsia 2015;56:841–848.
11. Yuan H, Low CM, Moody OA, et al. Ionotropic GABA and glutamate receptor mutations and human neurologic diseases. Mol Pharmacol 2015;88:203–217.
12. Helbig KL, Farwell Hagman KD, Shinde DN, et al. Diagnostic exome sequencing provides a molecular diagnosis for a significant proportion of patients with epilepsy. Genet Med 2016;18:898–905.
13. Lemke JR, Geider K, Helbig KL, et al. Delineating the GRIN1 phenotypic spectrum: a distinct genetic NMDA receptor encephalopathy. Neurology 2016;86:2171–2178.
14. Zehavi Y, Mandel H, Zehavi A, et al. De novo GRIN1 mutations: an emerging cause of severe early infantile encephalopathy. Eur J Med Genet 2017;60:317–320.
15. Fry AE, Fawcett KA, Zelnik N, et al. De novo mutations in GRIN1 cause extensive bilateral polymicrogyria. Brain 2018;141:698–712.
16. XiangWei W, Jiang Y, Yuan H. De novo mutations and rare variants occurring in NMDA receptors. Curr Opin Physiol 2018;2:27–35.
17. Richards S, Aziz N, Bale S, et al. Standards and guidelines for the interpretation of sequence variants: a joint consensus recommendation of the American College of Medical Genetics and Genomics and the Association for Molecular Pathology. Genet Med 2015;17:405–424.
18. Chen W, Tankovic A, Burger PB, et al. Functional evaluation of a de novo GRIN2A mutation identified in a patient with profound global developmental delay and refractory epilepsy. Mol Pharmacol 2017;91:317–330.
19. XiangWei W, Kannan V, Xu Y, et al. Heterogeneous clinical and functional features of GRIN2D-related developmental and epileptic encephalopathy. Brain 2019;142:3009–3027.
20. Yuan H, Erreger K, Dravid SM, Traynelis SF. Conserved structural and functional control of N-methyl-D-aspartate receptor gating by transmembrane domain M3. J Biol Chem 2005;280:29708–29716.
21. Jones KS, VanDongen HM, VanDongen AM. The NMDA receptor M3 segment is a conserved transduction element coupling ligand binding to channel opening. J Neurosci 2002;22:2044–2053.
22. Ogden KK, Chen W, Swanger SA, et al. Molecular mechanism of disease-associated mutations in the pre-M1 helix of NMDA receptors and potential rescue pharmacology. PLoS Genet 2017;13:e1006536.
23. Swanger S, Chen W, Wells G, et al. Mechanistic insight into NMDA receptor dysregulation by rare variants in the

© 2021 The Authors. *Annals of Clinical and Translational Neurology* published by Wiley Periodicals LLC on behalf of American Neurological Association

GluN2A and GluN2B agonist binding domains. Am J Hum Genet 2016;99:1261–1280.
24. Chang HR, Kuo CC. The activation gate and gating mechanism of the NMDA receptor. J Neurosci 2008;28:1546–1556.
25. Sobolevsky AI, Rosconi MP, Gouaux E. X-ray structure, symmetry and mechanism of an AMPA-subtype glutamate receptor. Nature 2009;462:745–756.
26. Li D, Yuan H, Ortiz-Gonzalez XR, et al. GRIN2D recurrent de novo dominant mutation causes a severe epileptic encephalopathy treatable with NMDA receptor channel blockers. Am J Hum Genet 2016;99:802–816.
27. Mullier B, Wolff C, Sands ZA, et al. GRIN2B gain of function mutations are sensitive to radiprodil, a negative allosteric modulator of GluN2B-containing NMDA receptors. Neuropharmacology 2017;123:322–331.
28. Platzer K, Yuan H, Schutz H, et al. GRIN2B encephalopathy: novel findings on phenotype, variant clustering, functional consequences and treatment aspects. J Med Genet 2017;54:460–470.
29. Amador A, Bostick CD, Olson H, et al. Modelling and treating GRIN2A developmental and epileptic encephalopathy in mice. Brain 2020;143:2039–2057.
30. Chez MG, Burton Q, Dowling T, et al. Memantine as adjunctive therapy in children diagnosed with autistic spectrum disorders: an observation of initial clinical response and maintenance tolerability. J Child Neurol 2007;22:574–579.
31. Erickson CA, Posey DJ, Stigler KA, et al. A retrospective study of memantine in children and adolescents with pervasive developmental disorders. Psychopharmacology 2007;191:141–147.
32. Camp CR, Yuan H. GRIN2D/GluN2D NMDA receptor: unique features and its contribution to pediatric developmental and epileptic encephalopathy. Eur J Paediatr Neurol 2020;24:89–99.
33. Kearney JA. Precision medicine: NMDA receptor-targeted therapy for GRIN2D encephalopathy. Epilepsy Curr 2017;17:112–114.
34. Karakas E, Furukawa H. Crystal structure of a heterotetrameric NMDA receptor ion channel. Science 2014;344:992–997.
35. Lee CH, Lü W, Michel JC, et al. NMDA receptor structures reveal subunit arrangement and pore architecture. Nature 2014;511:191–197.

Supporting Information

Additional supporting information may be found online in the Supporting Information section at the end of the article.

Table S1. Nitrocefin absorbance (optical density, O.D.) versus time course are indicated for HEK cells transfected with the WT β-lac-GluN1 and β-lac-GluN1-M641I when co-expressed with GluN2A.
Table S2. Nitrocefin absorbance (optical density, O.D.) versus time course are indicated for HEK cells transfected with the WT β-lac-GluN1 and β-lac-GluN1-M641I when co-expressed with GluN2B.
Table S3. The slopes of O.D. versus time were averaged as percentages of the WT NMDAR for the ratio of surface/total levels.
Table S4. Calculation of synaptic and non-synaptic charge transfer.

 © 2021 The Authors. *Annals of Clinical and Translational Neurology* published by Wiley Periodicals LLC on behalf of American Neurological Association